

Flavor-changing top quark rare decays in the Bestest Little Higgs model

T. Cisneros-Pérez^{*} and M. A. Hernández-Ruíz[†]

*Unidad Académica de Ciencias Químicas, Universidad Autónoma de Zacatecas
Apartado Postal C-585, 98060 Zacatecas, México.*

A. Gutiérrez-Rodríguez[‡] and E. Cruz-Albaro[§]

*Facultad de Física, Universidad Autónoma de Zacatecas
Apartado Postal C-580, 98060 Zacatecas, México.*

In this paper, we study the effects of the parameters of the Bestest Little Higgs (BLH) model on the flavor-changing top quark rare decays. We include new terms of flavor mixing between Standard Model (SM) light quarks and heavy fermions and bosons of the BLH model. We calculate the one-loop contributions of heavy quarks (B), new bosons (W'^{\pm}) and new scalars (H^{\pm}, ϕ^{\pm}), and we show that the decays $t \rightarrow qV$ and $t \rightarrow qh^0$, where $q = c, u$ and $V = \gamma, Z, g$, are improved respect to its relatives in the SM, except for the gluon. Of the processes analyzed, the ones that show the best sensitivity are $Br(t \rightarrow cZ) \sim 10^{-5}$, $Br(t \rightarrow c\gamma) \sim 10^{-6}$ and $Br(t \rightarrow ch^0) \sim 10^{-8}$, in the appropriate parameter space of the BLH model. Our study complements others studies on the flavor-changing top quark rare decays.

I. INTRODUCTION

The top quark is considered the principal connection with new physics beyond the SM (BSM) because it is the heaviest elementary particle known in nature; on the other hand, the Higgs boson can be used for extended mechanisms on to electroweak symmetry breaking (EWSB). These two ingredients have been used in many extensions of the SM: two-Higgs-doublet models [1–3], left-right models [4][5], SUSY [6–8], 331 models [9][10], etc. Experimentally, the copious production of top quarks at the Large Hadron Collider (LHC) in collisions of pp at a center-of-mass energy of 13 TeV [11–13] gives an important opportunity in the experimental measurements for the mentioned models. New facilities like the Forward Physics Facility (FPF) [14] at the LHC will allow a suite of far-forward experiments during the High-Luminosity (HL) era, such as heavy particles detection and rare processes measurements, proposed in various BSM. At the moment, theoretical analysis and experiments of flavor changing neutral currents (FCNC) [15–21] are of great interest due to the relation with the Cabibbo-Kobayashi-Maskawa (CKM) matrix [22] and the seek of new sources of CP violation [23] BSM [24]. There are relevant studies about this in the little Higgs models (LH), mainly in the Littlest Higgs Model with T-parity (LHT) [25][26][27]. In the SM and BSM, the top quark FCNC processes [28–37] could be highly suppressed [38] at the one-loop level by the Glashow-Iliopoulos-Maiani (GIM) mechanism [39], but in extended models, we do not have this restriction at one-loop contributions from heavy fermions and bosons partners. The BLH [40]

model improves several issues from former LH models, like the precision constraint theme, by including a custodial $SU(2)$ symmetry and also a second non-linear sigma field that couples only to the gauge bosons that inspired a possible relation with dark matter [41]. However, there has yet to be a study of FCNC top quark decays in the BLH model in the literature, although it may offer another test for constraints in its parameter space and new physics.

The paper is organized as follows: In Section II, we do an introduction to the BLH model, which is considered one parameter space, and we detail the flavor mixing terms that we have added. Section III showed the valid diagrams for the top quark rare decays in the BLH model, the amplitudes, and the cases for the CKM-like matrix we chose; finally, the graphics of the branchings ratios for the top quark rare decays. We summarize our conclusions in Section IV. We present the Feynman rules of the BLH model that we use in this paper in Appendix A. Appendix B contains the generalized amplitudes of the processes top quark rare.

II. A BRIEF REVIEW OF THE BLH MODEL

The BLH model arises from a symmetry group $SO(6)_A \times SO(6)_B$ that breaks at the scale f towards $SO(6)_V$ when the non-linear sigma field Σ acquires a VEV, $\langle \Sigma \rangle = 1$. There are now 15 pseudo-Nambu Goldstone bosons parameterized by the electroweak triplet ϕ^a ($a = 1, 2, 3$) with zero hypercharges and the triplet η^a where (η_1, η_2) form a complex singlet with hypercharge and η_3 is a real singlet,

$$\Sigma = e^{i\Pi/f} e^{2i\Pi_h/f} e^{i\Pi/f}, \quad (1)$$

^{*} tzihue@gmail.com

[†] maria.hernandez@uaz.edu.mx

[‡] alexgu@fisica.uaz.edu.mx

[§] elicruzalbaro88@gmail.com

$$\Pi = \begin{pmatrix} \phi_a T_L^a + \eta_a T_R^a & 0 & 0 \\ 0 & 0 & i\sigma/\sqrt{2} \\ 0 & -i\sigma/\sqrt{2} & 0 \end{pmatrix}, \quad (2)$$

$$\Pi_h = \begin{pmatrix} 0_{4 \times 4} & h_1 & h_2 \\ -h_1^T & 0 & 0 \\ -h_2^T & 0 & 0 \end{pmatrix}. \quad (3)$$

σ is a real scalar field necessary to produce a collective quartic coupling [40]. $T_{L,R}^a$ ($a = 1, 2, 3$) are the generators of $SU(2)_L$ and $SU(2)_R$. The second non-linear sigma field Δ from a global symmetry $SU(2)_C \times SU(2)_D$ is broken to a diagonal $SU(2)$ at the scale $F > f$ when develops a VEV, $\langle \Delta \rangle = 1$, this one is connected with Σ in such a way that the diagonal subgroup of $SU(2)_A \times SU(2)_B \subset SO(6)_A \times SO(6)_B$ is identified as the SM $SU(2)_L$. Besides, the diagonal combination $SU(2)_{RA} \times SU(2)_{RB} \subset SO(6)_A \times SO(6)_B$ is gauged by the hypercharge $U(1)_Y$. Including Δ contributes to the heavy gauge boson content of the BLH model like Z' and W'^{\pm} with masses proportional to $f^2 + F^2$. We chose that the components h_{11} and h_{21} acquires VEV's and to define the β angle such that,

$$\tan \beta = \frac{\langle h_{11} \rangle}{\langle h_{21} \rangle} = \frac{v_1}{v_2} = \frac{m_2}{m_1}, \quad (4)$$

where $m_1, m_2 > 0$ are masses related with the masses m_4, m_5 and m_6 in the scalar potential of the theory [40]. The VEV of the SM is linked with v_1 and v_2 in the form

$$\begin{aligned} v^2 &= v_1^2 + v_2^2 \\ &= \frac{1}{\lambda_0} \left(\frac{m_1^2 + m_2^2}{m_1 m_2} \right) (B_\mu - m_1 m_2) \\ &\simeq (246 \text{ GeV})^2, \end{aligned} \quad (5)$$

where B_μ and λ_0 comes from the scalar potential too. The EWSB in the model requires the bound $B_\mu > m_1 m_2$, i.e., so that the potential has a minimum, and $\lambda_0 \neq 0$ is the fundamental condition for the collective symmetry breaking. After the EWSB, the scalar sector [40][42] produces massive states of h^0 (SM Higgs), A^0 , H^\pm and H^0 , with masses

$$m_{G^0}^2 = m_{G^\pm}^2 = 0, \quad (6)$$

$$m_{A^0}^2 = m_{H^\pm}^2 = m_1^2 + m_2^2, \quad (7)$$

$$m_{h^0, H^0}^2 = \frac{B_\mu}{\sin 2\beta} \quad (8)$$

$$\mp \sqrt{\frac{B_\mu^2}{\sin^2 2\beta} - 2\lambda_0 \beta_\mu v^2 \sin 2\beta + \lambda_0^2 v^4 \sin^2 2\beta}$$

where (G^0, G^\pm) are Goldstone bosons who are eaten to give masses to W^\pm, Z bosons of the SM.

A. Gauge boson sector

The gauge kinetic terms are given by the Lagrangian [40]

$$\mathcal{L} = \frac{f^2}{8} \text{Tr} (D_\mu \Sigma^\dagger D^\mu \Sigma) + \frac{F^2}{4} \text{Tr} (D_\mu \Delta^\dagger D^\mu \Delta), \quad (9)$$

where $D_\mu \Sigma$ and $D_\mu \Delta$ are covariant derivatives.

The masses of the gauge bosons are given by [43]

$$m_\gamma^2 = 0, \quad (10)$$

$$\begin{aligned} m_{Z^0}^2 &= \frac{1}{4} v^2 (g^2 + g'^2) - (g^2 + g'^2) \\ &\times \left(2 + \frac{3f^2}{f^2 + F^2} (s_g^2 - c_g^2) \frac{v^4}{48f^2} \right), \end{aligned} \quad (11)$$

$$\begin{aligned} m_W^2 &= \frac{1}{4} g^2 v^2 \\ &- g^2 \left(2 + \frac{3f^2}{f^2 + F^2} (s_g^2 - c_g^2) \frac{v^4}{48f^2} \right), \end{aligned} \quad (12)$$

$$\begin{aligned} m_{Z'}^2 &= \frac{1}{4} (g_A^2 + g_B^2) (f^2 + F^2) - \frac{1}{4} g^2 v^2 \\ &+ \left(2g^2 + \frac{3f^2}{f^2 + F^2} \right. \end{aligned} \quad (13)$$

$$\left. \times (g^2 + g'^2) (s_g^2 - c_g^2) \frac{v^4}{48f^2} \right), \quad (14)$$

$$m_{W'}^2 = \frac{1}{4} (g_A^2 + g_B^2) (f^2 + F^2) - M_W^2, \quad (15)$$

where g' is the coupling of $U(1)_Y$, and g of the $SU(2)_L$ is related with the $SU(2)_A \times SU(2)_B$ couplings g_A and g_B by

$$g = \frac{g_A g_B}{\sqrt{g_A^2 + g_B^2}}, \quad (16)$$

$$s_g = \sin \theta_g = \frac{g_A}{\sqrt{g_A^2 + g_B^2}}, \quad (17)$$

$$c_g = \cos \theta_g = \frac{g_B}{\sqrt{g_A^2 + g_B^2}}, \quad (18)$$

here, θ_g is the mixing angle such that $g_A = g_B$ implies $\tan \theta_g = 1$.

B. Fermion sector

The fermion sector of the BLH model is ruled by the Lagrangian [40]

$$\begin{aligned} \mathcal{L}_t &= y_1 f Q^T S \Sigma SU^c + y_2 f Q_a'^T \Sigma U^c \\ &+ y_3 f Q^T \Sigma U_5'^c + y_b f q_3^T (-2i T_R^3 \Sigma) U_b^c + \text{h.c.} \end{aligned} \quad (19)$$

where (Q, Q') and (U, U') are multiplets of $SO(6)_A$ and $SO(6)_B$, respectively. S is an operator of symmetry, (y_1, y_2, y_3) are Yukawa couplings and (q_3, U_b^c) in the last term, Eq. (19), contains information about bottom

quark. The BLH model is focused on the quark sector and proposes six heavy partner quarks: T , T^5 , T^6 , $T^{2/3}$, $T^{5/3}$ and B with masses [40]

$$m_T^2 = (y_1^2 + y_2^2)f^2 \quad (20)$$

$$+ \frac{9v_1^2 y_1^2 y_2^2 y_3^2}{(y_1^2 + y_2^2)(y_2^2 - y_3^2)},$$

$$m_{T^5}^2 = (y_1^2 + y_3^2)f^2 \quad (21)$$

$$- \frac{9v_1^2 y_1^2 y_2^2 y_3^2}{(y_1^2 + y_3^2)(y_2^2 - y_3^2)},$$

$$m_{T^6}^2 = m_{T^{2/3}}^2 = m_{T^{5/3}}^2 = y_1^2 f^2, \quad (22)$$

$$m_B^2 = (y_1^2 + y_2^2)f^2. \quad (23)$$

where the Yukawa couplings in the quark sector Lagrangian [40] must satisfy $0 < y_i < 1$. The masses of t and b are generated too by Yukawa couplings y_t and y_b [42]

$$m_t^2 = y_t^2 v_1^2, \quad (24)$$

$$m_b^2 = y_b^2 v_1^2 - \frac{2y_b^2}{3\sin^2\beta} \frac{v_1^4}{f^2}. \quad (25)$$

The coupling y_t is part of the measure of fine-tuning in the BLH model, Ψ , defined by [42]

$$\Psi = \frac{27f^2}{8\pi^2 v^2 \lambda_0 \cos^2\beta} \frac{|y_1|^2 |y_2|^2 |y_3|^2}{|y_2|^2 - |y_3|^2} \log \frac{|y_1|^2 + |y_2|^2}{|y_1|^2 + |y_3|^2}. \quad (26)$$

The allowable values for this equation are $\Psi \approx 1$, to avoid the fine-tuning [40].

C. Parameter space of the BLH model

We use the parameter space such that they are consistent with the Eqs. (7), (8) and (26), and the conditions $h^0 = 125.46$ GeV [44], $\lambda_0 < 4\pi$, $\tan\beta \gtrsim 1$ and [43]

$$(\tan\beta)^2 < -1 \quad (27)$$

$$+ \frac{2 + \left(1 - \frac{m_{H^0}^2}{m_{A^0}^2}\right)^{\frac{1}{2}} \left(1 - \frac{m_{H^0}^2}{4\pi v^2}\right)^{\frac{1}{2}}}{\frac{m_{H^0}^2}{m_{A^0}^2} \left(1 + \frac{m_{A^0}^2 - m_{H^0}^2}{4\pi v^2}\right)}.$$

In Table I, we show the first parameters. The BLH model also consider the mixing angle α between h^0 and H^0 ,

$$\tan\alpha = \frac{1}{B_\mu - \lambda_0 v^2 \sin 2\beta} \left(B_\mu \cot 2\beta \right. \quad (28)$$

$$\left. + \sqrt{\frac{B_\mu^2}{\sin^2 2\beta} - 2\lambda_0 B_\mu v^2 \sin 2\beta + \lambda_0^2 v^4 \sin^2 2\beta} \right).$$

In this model, the mass m_4 is considered a free parameter in terms of which the masses ϕ^0 and η^0 are defined [40],

$$m_{\phi^0} = m_{\eta^0} \approx m_4, \quad (29)$$

these two terms have 1-loop corrections that can be discarded. In the same way, masses of ϕ^\pm and η^\pm receives small 1-loop corrections such that [40, 42, 43]

$$m_{\phi^\pm} = m_{\eta^\pm} \approx m_4. \quad (30)$$

We show a second set of value parameters in Table II. In this study, we have used only the fields (W^\pm, ϕ^\pm, H^\pm) and the heavy quark B inside the loop of the calculated decays because the model is restricted about couplings with the light quarks.

Table I: BLH model parameters.

Parameter				Unit
1.35	\leq	β	\leq	1.49 rad
1	\leq	λ_0	$<$	4π -
0.3287	\leq	y_3	\leq	0.3374 -
1	\leq	Ψ	\leq	3 -
307.25	\leq	m_{A^0}	\leq	1693.04 GeV
916.1	\leq	m_{H^0}	\leq	1900.33 GeV

Table II: BLH model parameters.

Parameter				Unit
3000	\leq	F	\leq	5000 GeV
67.29	\leq	m_1	\leq	136.64 GeV
299.79	\leq	m_2	$<$	1687.52 GeV
-0.1783	\leq	α	\leq	0.04722 rad
182677	\leq	B_μ	\leq	291763 -
$m_{\phi^\pm} = m_{\eta^\pm}$				800 GeV

D. Flavor mixing in the BLH model

The BLH model is flavor-conserving; however, authors emphasize the possibility of changing their flavor structure [40]. We have modified such structure most simply by adding two terms to the Lagrangian (19)

$$y_B f q_1 (-2iT_R^2 \Sigma) d_B^c, \quad y_B f q_2 (-2iT_R^2 \Sigma) d_B^c \quad (31)$$

where y_B , in terms of (y_1, y_2) , is the Yukawa coupling of heavy B quark, q_1 and q_2 are multiplets of light SM quarks

$$q_1^T = \frac{1}{\sqrt{2}}(-u, iu, d, id, 0, 0), \quad (32)$$

$$q_2^T = \frac{1}{\sqrt{2}}(-c, ic, s, is, 0, 0),$$

and d_B^c is the new multiplet that we have introduced

$$d_B^{cT} = (0, 0, 0, 0, B, 0). \quad (33)$$

This allows us the mixing between scalars fields (H^\pm, ϕ^\pm) and the B with the (u, c, d, s) quarks, which notably increase the phenomenology with the BLH model. The

Lagrangian (19) keeps its gauge invariance, and the new terms do not mix with heavy partners of the top quark. To acquire the mix with the heavy gauge bosons W'^{\pm} we follow the same way by adding a new term of mixing,

$$q_3^T = \frac{1}{\sqrt{2}}(0, 0, B, iB, 0, 0), \quad (34)$$

to the Lagrangian of gauge-fermion interactions [42]

$$\begin{aligned} \mathcal{L} = & iQ^\dagger \bar{\sigma}^\mu D_\mu Q + iQ'_a{}^\dagger \bar{\sigma}^\mu Q'_a - iU^{c\dagger} \sigma^\mu D_\mu U^c \\ & - iU'^{c\dagger} \sigma^\mu \mu U'^c - iU_b^{c\dagger} \tau^\mu D_\mu U_b^c \\ & + iq_i^\dagger \bar{\sigma}^\mu D_\mu q_i + iu_i^{c\dagger} \bar{\sigma}^\mu D_\mu u_i^c, \end{aligned} \quad (35)$$

such that we have

$$i\bar{q}_3 \bar{\sigma}^\mu D_\mu q_1, \quad i\bar{q}_3 \bar{\sigma}^\mu D_\mu q_2 \quad (36)$$

where (q_1, q_2) are the same that Eqs. (32), $\bar{\sigma}^\mu = -\sigma^\mu$ are the Pauli matrix and D_μ contains information about (W^\pm, W'^\pm) . The extended Lagrangian from (35) is gauge invariant and does not produce a mix with the heavy partners of the top quark.

III. PHENOMENOLOGY OF RARE TOP QUARK DECAYS

The valid diagrams for $t \rightarrow qV$ and $t \rightarrow qh^0$ where $q = (u, c)$ and $V = (Z, \gamma, g)$ are showed in Figs. (1) and (2). The scalar fields η^\pm do not have enough couplings for anyone of the diagrams, and they are not present in this work. The full amplitudes are shown in appendix B. We have thirty-six amplitudes that we have calculated using the Mathematica packages FeynCalc [45] and Package X [46]. Each amplitude of the decay $t \rightarrow qV$ has the structure

$$\mathcal{M}^\mu = \bar{u}(p_j) (F_1 p_i^\mu \mathbf{1} + F_2 p_i^\mu \gamma^5 + F_3 \gamma^\mu + F_4 \gamma^\mu \gamma^5) u(p_i), \quad (37)$$

The form factors (F_1, F_2, F_3, F_4) include masses and momenta of the external and internal quarks and gauge bosons of the BLH model and the SM of the Passarino-Veltman scalar functions. In the case, $t \rightarrow qh^0$, each amplitude has a different structure

$$\mathcal{M}^\mu = \bar{u}(p_j) (f_1 + f_2 \gamma^5) u(p_i), \quad (38)$$

$f_{1,2}$ contains terms from the BLH model and SM with Passarino-Veltman scalar functions.

A. Cases for the CKM matrix in the BLH model

The eigenstates of mass of the BLH model have not necessarily aligned with the eigenstates of the SM. This

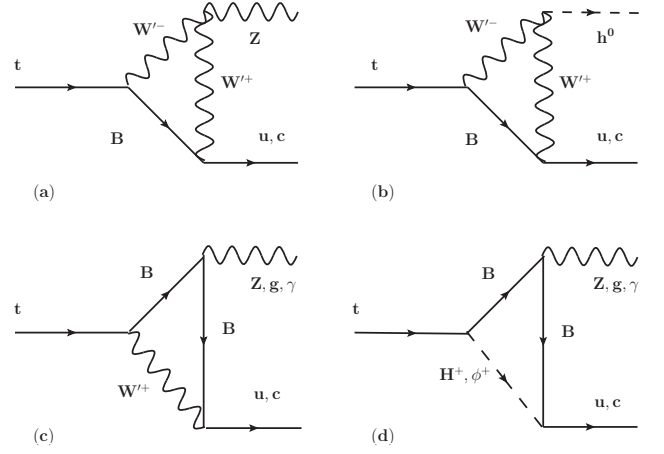


Fig. 1: Feynman diagrams for the flavor-changing top quark rare decays in the BLH model considered in this paper: $t \rightarrow qV$ and $t \rightarrow qh^0$ vertices, with $V = \gamma, Z, g$ and $q = u, c$.

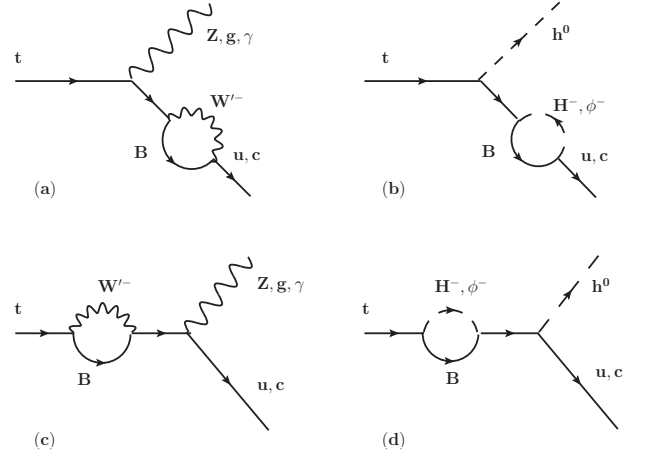


Fig. 2: Feynman diagrams for the flavor-changing top quark rare decays in the BLH model considered in this paper: $t \rightarrow qV$ and $t \rightarrow qh^0$ vertices, with $V = \gamma, Z, g$ and $q = u, c$.

idea has raised the CKM-like matrices in extended models of the SM [25][26][27]. We need two CKM-like unitary matrices

$$V_{Hu}, V_{Hd} \quad (39)$$

such that

$$V_{CKM} = V_{Hu}^\dagger V_{Hd}. \quad (40)$$

Actually, we know V_{CKM} therefore $V_{Hd} = V_{Hu} V_{CKM}$. The matrices in (39) parameterize flavor violating interactions between SM fermions (u, c) and bosons (Z, γ, g, h^0), and BLH model fermion B mediated by $(W'^{\pm}, H^{\pm}, \phi^{\pm})$, in this paper. We can generalize the CKM extended matrix like the product of three rotations

matrices [25][47]

$$V_{Hd} = \begin{pmatrix} 1 & 0 & 0 \\ 0 & c_{23}^d & s_{23}e^{-i\delta_{23}^d} \\ 0 & -s_{23}e^{i\delta_{23}^d} & c_{23}^d \end{pmatrix} \quad (41)$$

$$\times \begin{pmatrix} c_{13}^d & 0 & s_{13}e^{-i\delta_{13}^d} \\ 0 & 1 & 0 \\ -s_{13}e^{i\delta_{13}^d} & 0 & c_{13}^d \end{pmatrix} \quad (42)$$

$$\times \begin{pmatrix} c_{12}^d & s_{12}e^{-i\delta_{12}^d} & 0 \\ -s_{12}e^{i\delta_{12}^d} & c_{12}^d & 0 \\ 0 & 0 & 1 \end{pmatrix}. \quad (43)$$

Where the c_{ij}^d and s_{ij}^d are in terms of the angles $(\theta_{12}, \theta_{23}, \theta_{13})$ and the phases $(\delta_{12}, \delta_{23}, \delta_{13})$. We choose two cases:

Case I. $V_{Hd} = \mathbf{1}$, this implies $V_{Hu} = V_{CKM}^\dagger$.

Case II. $s_{23}^d = 1/\sqrt{2}$, $s_{12}^d = s_{13}^d = 0$, $\delta_{12}^d = \delta_{23}^d = \delta_{13}^d = 0$.

The first case produces suppressed branchings ratios below the second case. For this reason, we use Case II in our numerical calculation.

B. Branching ratios for the reactions $t \rightarrow qV$ and $t \rightarrow qh^0$ in the BLH model

The Branching ratios for the reactions $t \rightarrow qV$ and $t \rightarrow qh^0$ in the framework of the BLH model receive contributions from the diagrams at the one-loop level, as shown in Figs. (1)-(2), vector, fermion, and scalar contributions. Therefore, in this work, we study the contribution at the one-loop level, as well as the effects of the parameters from the BLH model on the branching ratios of the reactions $t \rightarrow qV$ and $t \rightarrow qh^0$ with $V = Z, \gamma, g$, and $q = u, c$, respectively, using the Feyn-Calcul [45] and Package X [46] toolkit.

To carry out our study, we apply the parameter space of the BLH model reported in Refs. [48–50], which are summarized in Tables I and II of Subsection II C. The parameter space, given by Tables I and II, is more restrictive but concordantly with the SM parameters and offers optimum branching ratios. In addition, we use Case II, mentioned in Subsection III A, for our analysis, where $s_{23}^d = 1/\sqrt{2}$, $s_{12}^d = s_{13}^d = 0$, $\delta_{12}^d = \delta_{23}^d = \delta_{13}^d = 0$.

It is worth mentioning that the mass of the heavy bottom quark B [51] is given by the relation $m_B = \sqrt{y_1^2 + y_2^2}f$, where $y_1 = 0.7$, $y_2 = 0.9$, while the masses of the bosons ϕ^\pm, H^\pm , depending on the parameters m_4 and m_1, m_2 , respectively. To quantify the expected sensitivity on the branching ratios of the reactions $t \rightarrow qV$ and $t \rightarrow qh^0$, an advantage has been taken in this analysis, and it has been shown in the literature that the branching fractions can enhance significantly in models BSM.

Table III and Figs. (3)-(13), show the expected Branching ratios of the flavor-changing top quark rare de-

cays, through the decays channels $t \rightarrow qV$ and $t \rightarrow qh^0$, with $q = u, c$ and $V = \gamma, Z, g$ at the BLH model. The best sensitivity on the Branching ratios might reach up to the order of magnitude $\mathcal{O}(10^{-8} - 10^{-5})$. As can be seen from these tables and figures, the $t \rightarrow cZ$, $t \rightarrow c\gamma$, and $t \rightarrow ch^0$ decay channels have good sensitivities among the branching ratios reported in the literature.

The ATLAS Collaboration [52] at the LHC has studied the sensitivity for the flavor-changing top quark rare decays obtaining the following results $Br(t \rightarrow qZ) = 3.1 \times 10^{-4}$ and 6.1×10^{-5} with $\mathcal{L} = 10 \text{ fb}^{-1}$ and 100 fb^{-1} ; $Br(t \rightarrow q\gamma) = 4.1 \times 10^{-5}$ and 1.2×10^{-5} with $\mathcal{L} = 10 \text{ fb}^{-1}$ and 100 fb^{-1} ; $Br(t \rightarrow qg) = 1.3 \times 10^{-3}$ and 4.2×10^{-4} with $\mathcal{L} = 10 \text{ fb}^{-1}$ and 100 fb^{-1} , respectively. More recently, the ATLAS Collaboration [53] realized a search for flavor-changing neutral-current interactions of a top quark and a gluon in pp collisions at $\sqrt{s} = 13 \text{ TeV}$ with the ATLAS detector. The Branching ratios obtained are of the order of $Br(t \rightarrow u + g) < 0.61 \times 10^{-4}$ and $Br(t \rightarrow c + g) < 3.7 \times 10^{-4}$.

Table III: The branching ratios for the top-quark decays via flavor changing neutral current couplings at the BLH model.

	Br_{BLH}	Br_{BLH}
Decay	$f = 1000 \text{ GeV}$	$f = 3000 \text{ GeV}$
$t \rightarrow uZ$	3.5×10^{-10}	3.0×10^{-11}
$t \rightarrow u\gamma$	2.5×10^{-11}	2.2×10^{-12}
$t \rightarrow ug$	4.0×10^{-17}	4.2×10^{-20}
$t \rightarrow uh^0$	8.2×10^{-13}	5.9×10^{-15}
$t \rightarrow cZ$	3.7×10^{-5}	3.1×10^{-6}
$t \rightarrow c\gamma$	2.6×10^{-6}	2.3×10^{-8}
$t \rightarrow cg$	4.2×10^{-13}	4.5×10^{-16}
$t \rightarrow ch^0$	8.5×10^{-9}	6.2×10^{-11}

Others studies realized in the context of the littlest Higgs model with T-parity are reported in Refs. [26] and [27]. In Ref. [26] are reported Branching ratios of the order of $Br(t \rightarrow cg) \sim 10^{-2}$, $Br(t \rightarrow cZ) \sim 10^{-5}$, and $Br(t \rightarrow c\gamma) \sim 10^{-7}$, and similar results are obtained in Ref. [27]. It is worth mentioning that Ref. [38], is an exhaustive review on theoretical expectations and experimental detection of top flavor-changing neutral interactions in different models. A paper relatively recently [54], presents a study that analyzed the prospect of constraining the $Br(t \rightarrow ch^0)$ through top quark pair production at the 100 TeV FCC-hh. Their analysis can provide constraints on the branching ratio of the order of $Br(t \rightarrow ch^0) \approx \mathcal{O}(10^{-3})$.

Also, we incorporate the experimental branching ratios in Table V for comparison purposes.

Figs. (3)-(13) show the branching ratios of the reactions $t \rightarrow qV$ and $t \rightarrow qh^0$, where $q = c, u$ and $V = \gamma, Z, g$ as a function of the energy scale f of the BLH model. For our analysis, we consider the parameters of the BLH model given in Tables I and II.

Fig. (3) shows the branching ratios for four top quark decay modes $t \rightarrow uZ, u\gamma, ug, uh^0$ as a function of the f parameter. All the channels show a strong sensitivity concerning the energy scale f , and the branching ratios decrease as f increases. From this figure it can be seen that the channels $t \rightarrow uZ$ and $t \rightarrow u\gamma$ give a branching ratios of $\mathcal{O}(10^{-10} - 10^{-9})$ for $f \in [1000, 3000]$ GeV and $m_B = (1.14)f$.

Similarly, Fig. (4) shows the branching ratios for the channels $t \rightarrow cZ, c\gamma, cg, ch^0$ as a function of the free parameter $f \in [1000, 3000]$ GeV and $m_B = (1.14)f$. The channels that provide the highest branching ratios are $t \rightarrow cZ$ and $t \rightarrow c\gamma$ with branching ratios of the order of $\mathcal{O}(10^{-6} - 10^{-5})$, respectively. On the other hand, if we consider the branching ratios $Br(t \rightarrow cZ)$, $Br(t \rightarrow c\gamma)$, $Br(t \rightarrow cg)$, and $Br(t \rightarrow ch^0)$ as a function of the mass of the heavy bottom quark m_B with $f = 1000$ GeV fixed, we obtain branching ratios of the order of $\mathcal{O}(10^{-6} - 10^{-5})$ for the channels $t \rightarrow cZ$ and $t \rightarrow c\gamma$ as shown in Fig. (5). In addition, our analysis contemplates Figs. (6)-(13) which illustrate the branching ratios for the eight decay channels of the top quark, that is, $Br(t \rightarrow uZ, u\gamma, ug, uh^0)$ and $Br(t \rightarrow cZ, c\gamma, cg, ch^0)$ with the virtual particles $B, W'^{\pm}, H^{\pm}, \phi^{\pm}$ circulating in the loop. These figures show that the channels $Br(t \rightarrow cZ)$ and $Br(t \rightarrow c\gamma)$ with virtual ϕ^{\pm} give the highest contribution to the total branching ratios.

In the next Section, we present our conclusions on the flavor-changing top quark rare decays in the context of the BLH model.

Table IV: In the decoupling limit between the SM and the BLH model, we reproduce the predictions of the SM on the Branching ratios for $t \rightarrow qV$ and $t \rightarrow qh^0$ where $q = (u, c)$ and $V = (Z, \gamma, g)$.

Decay	Br_{SM}
$t \rightarrow uZ$	8×10^{-17}
$t \rightarrow u\gamma$	3.7×10^{-16}
$t \rightarrow ug$	3.7×10^{-14}
$t \rightarrow uh^0$	2×10^{-17}
$t \rightarrow cZ$	1×10^{-14}
$t \rightarrow c\gamma$	4.6×10^{-14}
$t \rightarrow cg$	4.6×10^{-12}
$t \rightarrow ch^0$	3×10^{-15}

Table V: Experimental upper limits on the $Br(t \rightarrow qV)$ and $Br(t \rightarrow qh^0)$ [53][55].

Decay	Br
$t \rightarrow qZ$	5×10^{-4}
$t \rightarrow q\gamma$	1.8×10^{-4}
$t \rightarrow ug$	0.61×10^{-4}
$t \rightarrow cg$	3.7×10^{-4}
$t \rightarrow uh^0$	1.2×10^{-3}
$t \rightarrow ch^0$	1.1×10^{-3}

IV. CONCLUSIONS

In this paper, we calculate and study the effects of the one-loop contributions from the heavy gauge bosons W'^{\pm} , heavy quark bottom B , and the new scalars H^{\pm}, ϕ^{\pm} predicted for the BLH model, as well as of the effect of the parameters from this model on the top quark rare decay processes $t \rightarrow qV$ and $t \rightarrow qh^0$.

Our results on the $Br(t \rightarrow qV)$ and $Br(t \rightarrow qh^0)$ are summarized in Table III and in Figs.(3)-(13). From this table and figures, it is clear that the largest contribution to the branching ratios comes from the channels $Br(t \rightarrow cZ) = 3.7 \times 10^{-5}$ and $Br(t \rightarrow c\gamma) = 2.6 \times 10^{-6}$ and $Br(t \rightarrow ch^0) = 8.5 \times 10^{-8}$ for the scale of breaking of the symmetry of the BLH model of $f = [1000, 3000]$ GeV.

It is worth mentioning that in the decoupling limit between the SM and the BLH model, our calculations consistently reproduce the predictions of the SM on the branching ratios of the flavor-changing top quark rare decays at the Bestest Little Higgs model $Br(t \rightarrow qV)$ and $Br(t \rightarrow qh^0)$ with $q = u, c$ and $V = Z, \gamma, g$, as shown in Table IV. In addition, our results reported in this paper are consistent with those reported in the literature, and in some cases, they predict higher branching ratios.

The rare decay modes $t \rightarrow cZ$ and $t \rightarrow c\gamma$ we have investigated in the present article could be measured with good sensitivity in the High Luminosity (HL) and High Energy (HE) era at the LHC [14], as well as in the Future Circular hadron-hadron Collider (FCC-hh). Future colliders of leptons such as the Compact Linear Collider (CLIC) [56, 57] and the muon Collider with HL and HE [58]. Given that the current and future colliders contemplate the physics of the top quark in their research programs.

In summary, in the present study, we analyze the prospect of constraining the $Br(t \rightarrow uZ, u\gamma, ug, uh^0)$ and $Br(t \rightarrow cZ, c\gamma, cg, ch^0)$ at the BLH model. In addition, this study represents the first estimate for a constraint on these couplings at the BLH model. Due to its theoretical and phenomenological characteristics, the BLH model is considered a good candidate for future experiments in the medium-term.

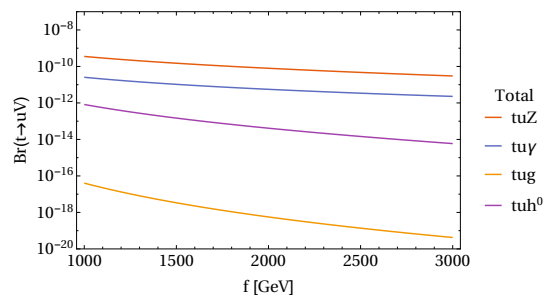


Fig. 3: Total contributions to $Br(t \rightarrow uZ, u\gamma, ug, uh^0)$ as a function of the scale of energy f , with $m_B = (1.14)f$ and $F = 5000$ GeV.

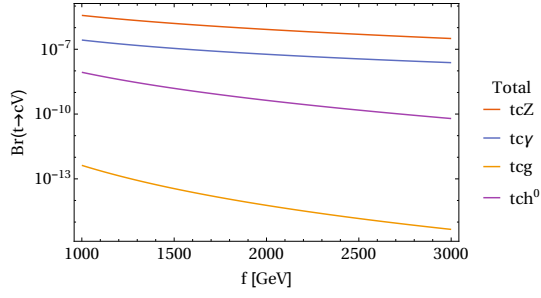


Fig. 4: Total contributions to $Br(t \rightarrow cZ, c\gamma, cg, ch^0)$ as a function of the scale of energy f , with $m_B = (1.14)f$ and $F = 5000$ GeV.

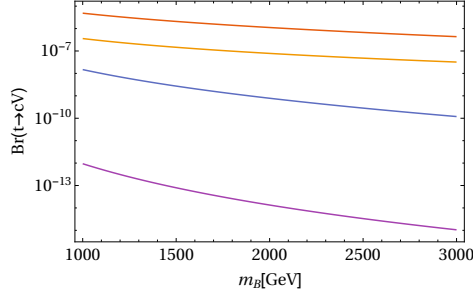


Fig. 5: Total contributions to $Br(t \rightarrow cZ, c\gamma, cg, ch^0)$ as a function of the mass of the heavy quark bottom B and $F = 5000$ GeV.

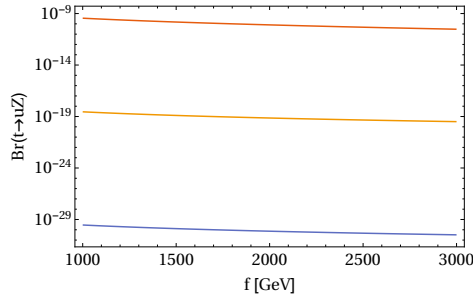


Fig. 6: Partials $Br(t \rightarrow uZ)$ with the virtual particles $B, W'^{\pm}, H^{\pm}, \phi^{\pm}$ circulating in the loop.

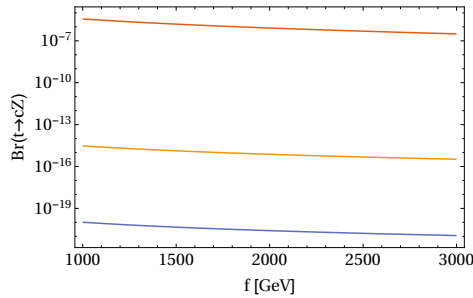


Fig. 7: Same as in Fig. (6), but for the $Br(t \rightarrow cZ)$.

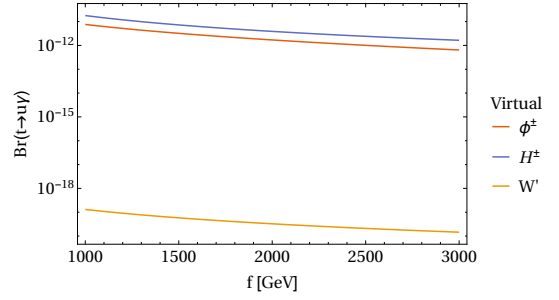


Fig. 8: Same as in Fig. (6), but for the $Br(t \rightarrow u\gamma)$.

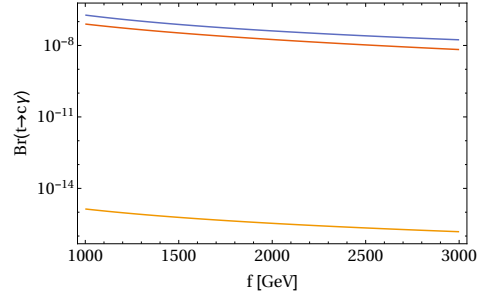


Fig. 9: Same as in Fig. (6), but for the $Br(t \rightarrow c\gamma)$.

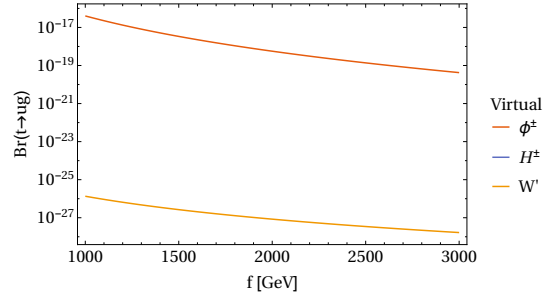


Fig. 10: Same as in Fig. (6), but for the $Br(t \rightarrow ug)$.

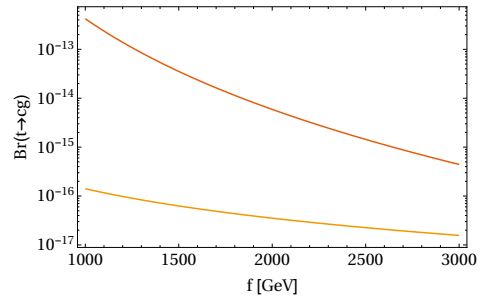


Fig. 11: Same as in Fig. (6), but for the $Br(t \rightarrow cg)$.

ACKNOWLEDGMENTS

A CONACYT Postdoctoral Fellowship has supported this work.

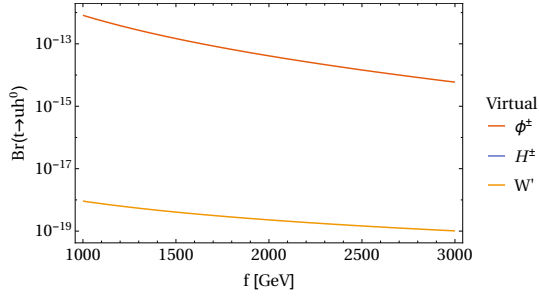


Fig. 12: Same as in Fig. (6), but for the $Br(t \rightarrow uh^0)$.

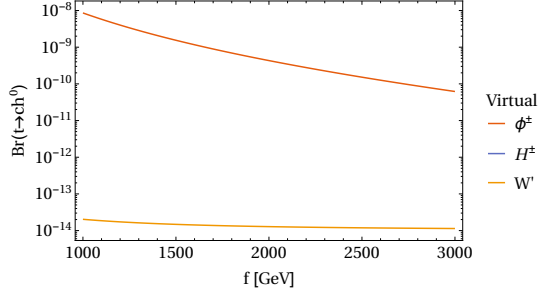


Fig. 13: Same as in Fig. (6), but for the $Br(t \rightarrow ch^0)$.

Appendix A: Feynman rules

In this Appendix, we derived and collected the Feynman rules for the BLH model necessary to calculate the flavor-changing top quark rare decays.

Tables VI-VIII summarized Feynman rules for the 3-point interactions fermion-fermion-scalar (FFS), fermion-fermion-gauge (FFV), gauge-gauge-gauge (VVV), and scalar-gauge-gauge (SVV) interactions.

Table VI: Essential Feynman rules in the BLH model for studying the flavor-changing top quark rare decays are the 3-point interactions fermion-fermion-scalar (FFS), fermion-fermion-gauge (FFV), gauge-gauge-gauge (VVV), and scalar-gauge-gauge (SVV) interactions.

Vertex	Rule
$W'^- \bar{B}t$	$-\frac{-igs_{\beta}v}{4\sqrt{2}f}A_y\gamma^{\mu}P_L(V_{Hu})$
$W'^- \bar{B}u$	$\frac{igg_A}{2\sqrt{2}q_B}\gamma^{\mu}P_L(V_{Hu})$
$W'^- \bar{B}c$	$\frac{igg_A}{2\sqrt{2}q_B}\gamma^{\mu}P_L(V_{Hu})$
$\phi^- \bar{B}t$	$F_a F_b (X_1 P_L + X_2 P_R)(V_{Hu})$
$\phi^- \bar{B}u$	$\frac{iFs_{\beta}^2 [m_u + m_B + (m_u - m_B)\gamma^5]}{2f\sqrt{2}\sqrt{f^2 + F^2}}(V_{Hu})$
$\phi^- \bar{B}c$	$\frac{iFs_{\beta}^2 [m_c + m_B + (m_c - m_B)\gamma^5]}{2f\sqrt{2}\sqrt{f^2 + F^2}}(V_{Hu})$
$H^- \bar{B}t$	$\frac{-3\sqrt{2}m_W c_{\beta} s_{\beta} y_1 y_2 y_3^2}{fg\sqrt{y_1^2 + y_2^2}(y_1^2 + y_3^2)}P_L(V_{Hu})$
$H^- \bar{B}u$	$\frac{gm_B s_{2\beta}}{4\sqrt{2}m_W}P_L(V_{Hu})$
$H^- \bar{B}c$	$\frac{gm_B s_{2\beta}}{4\sqrt{2}m_W}P_L(V_{Hu})$
$Z\bar{B}B$	$-\frac{ig}{6c_W}(3c_W^2 - 7s_W^2)\gamma^{\mu}$
$\gamma\bar{B}B$	$-\frac{1}{3}igs_W\gamma^{\mu}$
$Z_{q,\mu}W'_{k,\alpha}W'^+_{p,\beta}$	$igc_W[\delta_{\beta\mu}\Delta_1 + \delta_{\alpha\mu}\Delta_2 + \delta_{\alpha\beta}\Delta_3]$
$h^0W'^-W'^+$	$2gm_W s_{\alpha+\beta}$

Appendix B: Transition amplitudes

Here, we present the transition amplitudes to a one-loop level corresponding to the Feynman diagrams in Figs. (1) and (2), for the flavor-changing top quark rare decays. The amplitudes are summarized in Eqs. (B1)-(B8).

The amplitude of the diagram (a) of Fig. (1):

Table VII: Factors from Table VI.

Factor	Expression
A_y	$y_3(2y_1^2 - y_2^2)(y_1^2 + y_2^2)^2(y_1^2 + y_3^2)$
F_a	$\frac{y_3(2y_1^2 - y_2^2)}{(y_1^2 + y_3^2)\sqrt{y_1^2 + y_2^2}}$
F_b	$\frac{Fs_{\beta}}{2f\sqrt{2(f^2 + F^2)}}$
X_1	$A_1 + A_3 + A_6$
X_2	$A_2 + A_4 + A_5$

Table VIII: Factors from Table VI.

A_1	$\frac{-4m_W c_\beta^2 y_1 y_2 (y_1^2 + y_3^2)}{s_\beta y_3 (2y_1^2 - y_2^2)}$
A_2	$fg - y_1^8 - m_W s_\beta y_3 y_2^6 - 3y_2 y_1^4 (2y_1^2 - y_2^2) - y_1^6 (3y_2^2 + y_3^2) - y_1^2 y_2^4 (y_2^2 + 3y_3^2)$
A_3	$\frac{-4m_W y_1^3 y_2 y_3}{2y_1^2 - y_2^2}$
A_4	$\frac{8m_W y_1^3 (y_2^2 + y_3^2)}{2y_1^2 - y_2^2}$
A_5	$\frac{-4m_W y_1^3}{2y_1^2 - y_2^2}$
A_6	$\frac{4m_W y_1^3 y_2}{y_3 (2y_1^2 - y_2^2)}$
Δ_1	$p_\alpha - q_\alpha$
Δ_2	$q_\beta - k_\beta$
Δ_3	$k_\mu - p_\mu$

$$\begin{aligned}
\mathcal{M}_{1a}^\mu &= \int \frac{d^4 k}{(2\pi)^4} \bar{u}_j(p_j) (B_{W',Q}) \left[i \frac{\not{k} + m_B}{k^2 - m_B^2} \right] (B_{W',t}) \\
&\times \left[\frac{i}{(k - q - p_j)^2 - m_{W'}^2} \left(-g^{\alpha_3 \alpha_4} + \frac{(k - q - p_j)_{\alpha_3} (k - q - p_j)_{\alpha_4}}{m_{W'}^2} \right) \right] \\
&\times (Z_{W',W'}) \left[\frac{i}{(k - p_j)^2 - m_{W'}^2} \left(-g^{\alpha_1 \alpha_2} + \frac{(k - p_j)_{\alpha_1} (k - p_j)_{\alpha_2}}{m_{W'}^2} \right) \right] u_i(p_i), \quad (B1)
\end{aligned}$$

where the coefficients $B_{W',Q} = \{W'^- \bar{B}u, W'^- \bar{B}c\}$, $B_{W',t}$ and $Z_{W',W'}$ are the corresponding vertex.

The amplitude of diagram (b) of Fig. (1):

$$\begin{aligned}
\mathcal{M}_{1b}^\mu &= \int \frac{d^4 k}{(2\pi)^4} \bar{u}_j(p_j) (B_{W',Q}) \left[i \frac{\not{k} + m_B}{k^2 - m_B^2} \right] \\
&\times (B_{W',t}) \left[\frac{i}{(k - q - p_j)^2 - m_{W'}^2} \left(-g^{\alpha_3 \alpha_4} + \frac{(k - q - p_j)_{\alpha_3} (k - q - p_j)_{\alpha_4}}{m_{W'}^2} \right) \right] \\
&\times (h_{W',W'}^0) \left[\frac{i}{(k - p_j)^2 - m_{W'}^2} \left(-g^{\alpha_1 \alpha_2} + \frac{(k - p_j)_{\alpha_1} (k - p_j)_{\alpha_2}}{m_{W'}^2} \right) \right] u_i(p_i), \quad (B2)
\end{aligned}$$

where $h_{W',W'}^0 = h^0 W'^+ W'^-$.

The amplitude of the diagram (c) of Fig. (1):

$$\begin{aligned}
\mathcal{M}_{1c}^\mu &= \int \frac{d^4 k}{(2\pi)^4} \bar{u}_j(p_j) (B_{W',Q}) \left[i \frac{\not{k} - \not{p}_j + m_B}{(k - p_j)^2 - m_B^2} \right] \\
&\times (V_{B,B}) \left[i \frac{\not{k} - \not{q} - \not{p}_j + m_B^2}{(k - q - p_j)^2 - m_B^2} \right] (B_{W',t}) \quad (B3) \\
&\times \left[\frac{i}{k^2 - m_{W'}^2} \left(-g^{\alpha_1 \alpha_2} + \frac{k_{\alpha_1} k_{\alpha_2}}{m_{W'}^2} \right) \right] u_i(p_i),
\end{aligned}$$

where $V_{B,B} = \{Z\bar{B}B, g\bar{B}B, \gamma\bar{B}B\}$ are the vertex.

The amplitude of diagram (d) of Fig. (1):

$$\begin{aligned}
\mathcal{M}_{1d}^\mu &= \int \frac{d^4 k}{(2\pi)^4} \bar{u}_j(p_j) (B_{S,Q}) \left[\frac{i}{k^2 - m_S^2} \right] (B_{S,t}) \\
&\times \left[i \frac{\not{k} - \not{q} - \not{p}_j + m_B}{(k - q - p_j)^2 - m_B^2} \right] (V_{B,B}) \\
&\times \left[i \frac{\not{p}_j + m_t}{p_j^2 - m_t^2} \right] u_i(p_i) \quad (B4)
\end{aligned}$$

where $B_{S,Q} = \{B_{\phi^-,Q}, B_{H^-,Q}\}$ and $B_{S,t} = \{B_{\phi^-,t}, B_{H^-,t}\}$ are the vertex, and $m_S = \{m_\phi, m_{H^-}\}$ are the masses.

The amplitude of the diagram (a) of Fig. (2):

$$\begin{aligned}
\mathcal{M}_{2a}^\mu &= \int \frac{d^4 k}{(2\pi)^4} \bar{u}_j(p_j) (B_{W',Q}) \left[i \frac{\not{k} + m_B}{k^2 - m_B^2} \right] \\
&\times (B_{W',t}) \left[\frac{i}{(k - p_j)^2 - m_{W'}^2} \left(-g^{\alpha_1 \alpha_2} + \frac{(k - p_j)_{\alpha_1} (k - p_j)_{\alpha_2}}{m_{W'}^2} \right) \right] (V_{t,t}) \\
&\times \left[i \frac{\not{p}_j + m_t}{p_j^2 - m_t^2} \right] u_i(p_i), \quad (B5)
\end{aligned}$$

where $V_{t,t} = \{Z\bar{t}t, g\bar{t}t, \gamma\bar{t}t\}$ are the vertex.

The amplitude of diagram (b) of Fig. (2):

where $V_{Q,Q} = \{Z\bar{Q}Q, g\bar{Q}Q, \gamma\bar{Q}Q\}$.

$$\begin{aligned} \mathcal{M}_{2b}^\mu &= \int \frac{d^4k}{(2\pi)^4} \bar{u}_j(p_j) (B_{S,Q}) \left[i \frac{\not{k} + m_B}{k^2 - m_B^2} \right] \\ &\times (B_{S,t}) \left[\frac{i}{(k - p_j)^2 - m_S^2} \right] (h_{t,t}^0) \\ &\times \left[i \frac{\not{p}_j + m_t}{p_j^2 - m_t^2} \right] u_i(p_i), \end{aligned} \quad (\text{B6})$$

where $h_{t,t}^0 = h^0 \bar{t}t$.

The amplitude of the diagram (c) of Fig. (2):

$$\begin{aligned} \mathcal{M}_{2c}^\mu &= \int \frac{d^4k}{(2\pi)^4} \bar{u}_j(p_j) (V_{Q,Q}) \left[i \frac{\not{q} + \not{p}_j + m_Q}{(q + p_j)^2 - m_Q^2} \right] \\ &\times (B_{W',Q}) \left[i \frac{\not{k} + m_B}{k^2 - m_B^2} \right] (B_{W',t}) \\ &\times \left[\frac{i}{(k - q - p_j)^2 - m_S^2} \right] u_i(p_i), \end{aligned} \quad (\text{B7})$$

The amplitude of diagram (d) of Fig. (2):

$$\begin{aligned} \mathcal{M}_{2c}^\mu &= \int \frac{d^4k}{(2\pi)^4} \bar{u}_j(p_j) (h_{Q,Q}^0) \left[i \frac{\not{q} + \not{p}_j + m_Q}{(q + p_j)^2 - m_Q^2} \right] \\ &\times (B_{S,Q}) \left[i \frac{\not{k} + m_B}{k^2 - m_B^2} \right] (B_{S,t}) \\ &\times \left[\frac{i}{(k - q - p_j)^2 - m_B^2} \right] u_i(p_i). \end{aligned} \quad (\text{B8})$$

-
- [1] M. Schmaltz and D. Tucker-Smith, Little higgs theories, *Annu. Rev. Nucl. Part. Sci.* **55**, 229 (2005).
 - [2] N. Arkani-Hamed, A. G. Cohen, E. Katz, and A. E. Nelson, The littlest higgs, *Journal of High Energy Physics* **2002**, 034 (2002).
 - [3] A. Gutierrez-Rodriguez, Little Higgs Models: Dipole Moments of the ν_τ and Energy Scale f , *Int. J. Theor. Phys.* **54**, 236 (2015).
 - [4] M. Blanke, A. J. Buras, K. Gemmler, and T. Heidsieck, $\delta f = 2$ observables and $b \rightarrow x q \gamma$ decays in the left-right model: Higgs particles striking back, *Journal of High Energy Physics* **2012**, 1 (2012).
 - [5] R. Gaitán, O. G. Miranda, and L. G. Cabral-Rosetti, Rare top quark and higgs boson decays in alternative left-right symmetric models, *Phys. Rev. D* **72**, 034018 (2005).
 - [6] M. Drees and S. P. Martin, Implications of susy model building, arXiv [10.48550/arXiv.hep-ph/9504324](https://arxiv.org/abs/10.48550/arXiv.hep-ph/9504324) (1995).
 - [7] C. S. Li, R. Oakes, and J. M. Yang, Rare decays of the top quark in the minimal supersymmetric model, *Physical Review D* **49**, 293 (1994).
 - [8] C. W. L. Y. J. M. Z. M. Cao, Junjie Han, SUSY induced top quark FCNC decay $t \rightarrow ch$ after Run I of LHC, *The European Physical Journal C* **74**, 3058 (2014).
 - [9] F. Pisano and V. Pleitez, $SU(3) \otimes U(1)$ model for electroweak interactions, *Phys. Rev. D* **46**, 410 (1992).
 - [10] F. Larios, R. Martinez, and M. Perez, New physics effects in the flavor-changing neutral couplings of the top quark, *Int. J. Mod. Phys. A* **21**, 3473 (2006).
 - [11] A. M. Sirunyan, A. Tumasyan, W. Adam, F. Ambrogio, E. Asilar, T. Bergauer, J. Brandstetter, M. Dragicovic, J. Erö, A. E. Del Valle, *et al.*, Measurement of the production cross section, the top quark mass, and the strong coupling constant using dilepton events in pp collisions, *The European Physical Journal C* **79**, 1 (2019).
 - [12] T. A. collaboration, Search for top-quark decays $t \rightarrow qh$ with 36 fb^{-1} of pp collision data at $\sqrt{s} = 13 \text{ TeV}$ with the ATLAS detector, *Journal of High Energy Physics* **2019**, [10.1007/JHEP05\(2019\)123](https://arxiv.org/abs/10.1007/JHEP05(2019)123) (2019).
 - [13] T. et al. (CMS Collaboration), Search for flavor-changing neutral current interactions of the top quark and higgs boson in final states with two photons in proton-proton collisions at $\sqrt{s} = 13 \text{ TeV}$, *Phys. Rev. Lett.* **129**, 032001 (2022).
 - [14] J. L. Feng, F. Kling, M. H. Reno, J. Rojo, D. Soldin, L. A. Anchordoqui, J. Boyd, A. Ismail, L. Harland-Lang, K. J. Kelly, *et al.*, The forward physics facility at the high-luminosity LHC, *J. Phys. G: Nucl. Part. Phys.* **50**, 030501 (2023).
 - [15] N. F. Castro and K. Skovpen, Flavour-changing neutral scalar interactions of the top quark, *Universe* **8**, [10.3390/universe8110609](https://arxiv.org/abs/10.3390/universe8110609) (2022).
 - [16] J. Aebischer, A. J. Buras, M. Cerda-Sevilla, and F. De Fazio, Quark-lepton connections in Z' mediated FCNC processes: gauge anomaly cancellations at work, *Journal of High Energy Physics* **2020**, 1 (2020).
 - [17] J. Montaña Domínguez, B. Quezadas-Vivian, F. Ramírez-Zavaleta, and E. S. Tututi, Weak dipole moments of heavy fermions with flavor violation induced by Z' gauge bosons, *J. Phys. G* **49**, 075004 (2022), [arXiv:2206.07641 \[hep-ph\]](https://arxiv.org/abs/2206.07641).
 - [18] T. C. collaboration, Search for flavor-changing neutral current interactions of the top quark and the Higgs boson decaying to a bottom quark-antiquark pair at $\sqrt{s} = 13 \text{ TeV}$, *Journal of High Energy Physics* **2022**, [10.1007/JHEP02\(2022\)169](https://arxiv.org/abs/10.1007/JHEP02(2022)169) (2022).
 - [19] A. Collaboration *et al.*, Search for flavour-changing neutral current interactions of the top quark and the Higgs boson in events with a pair of τ -leptons in pp collisions at $\sqrt{s} = 13 \text{ TeV}$ with the ATLAS detector, arXiv

- 10.48550/arXiv.2208.11415 (2022).
- [20] Y.-B. Liu and S. Moretti, Probing the top-Higgs boson FCNC couplings via the $h \rightarrow \gamma\gamma$ channel at the HE-LHC and FCC-hh, *Phys. Rev. D* **101**, 075029 (2020).
 - [21] O. Ozsimsek, V. Ari, and O. Cakir, Investigating top-Higgs FCNC couplings at the FCC-hh, *Nuclear Physics B* **983**, 115908 (2022).
 - [22] M. Kobayashi and T. Maskawa, Cp-violation in the renormalizable theory of weak interaction, *Progress of theoretical physics* **49**, 652 (1973).
 - [23] M. Parkhari, M. Sayahi, S. Dadfar, and S. Zarrin, The possible contribution of B_s^0 meson decay into $X(3872)$ and $\phi(1020)$, *Phys. Lett. B* **839**, 137792 (2023).
 - [24] T. Kapoor and E. Kou, New physics search via CP observables in $B_s^0 \rightarrow \phi\phi$ decays with left- and right-handed Chromomagnetic operators 10.48550/arXiv.2303.04494 (2023), [arXiv:2303.04494 \[hep-ph\]](#).
 - [25] M. Blanke, A. J. Buras, A. Poschenrieder, S. Recksiegel, C. Tarantino, S. Uhlig, and A. Weiler, Another look at the flavour structure of the Littlest Higgs model with T-parity, *Physics Letters B* **646**, 253 (2007).
 - [26] H. Hong-Sheng, Flavor-changing top quark rare decays in the littlest Higgs model with T parity, *Physical Review D* **75**, 094010 (2007).
 - [27] J. Han, B. Yang, and J. Li, Revisiting rare top quark decays in the littlest Higgs Model with T-parity, *Int.J.Mod.Phys. A* **31**, 1650165 (2016).
 - [28] B. Mele, S. Petrarca, and A. Soddu, A New evaluation of the $t \rightarrow c h$ decay width in the standard model, *Phys. Lett. B* **435**, 401 (1998), [arXiv:hep-ph/9805498](#).
 - [29] J. J. Cao, G. Eilam, M. Frank, K. Hikasa, G. L. Liu, I. Turan, and J. M. Yang, SUSY-induced FCNC top-quark processes at the large hadron collider, *Phys. Rev. D* **75**, 075021 (2007), [arXiv:hep-ph/0702264](#).
 - [30] J. L. Diaz-Cruz, H.-J. He, and C. P. Yuan, Soft SUSY breaking, stop charm mixing and Higgs signatures, *Phys. Lett. B* **530**, 179 (2002), [arXiv:hep-ph/0103178](#).
 - [31] G. Eilam, A. Gemintern, T. Han, J. M. Yang, and X. Zhang, Top quark rare decay $t \rightarrow c h$ in R-parity violating SUSY, *Phys. Lett. B* **510**, 227 (2001), [arXiv:hep-ph/0102037](#).
 - [32] F. Larios, R. Martinez, and M. A. Perez, New physics effects in the flavor-changing neutral couplings of the top quark, *Int. J. Mod. Phys. A* **21**, 3473 (2006), [arXiv:hep-ph/0605003](#).
 - [33] K. Agashe, G. Perez, and A. Soni, Collider Signals of Top Quark Flavor Violation from a Warped Extra Dimension, *Phys. Rev. D* **75**, 015002 (2007), [arXiv:hep-ph/0606293](#).
 - [34] T. Han, R. D. Peccei, and X. Zhang, Top quark decay via flavor changing neutral currents at hadron colliders, *Nucl. Phys. B* **454**, 527 (1995), [arXiv:hep-ph/9506461](#).
 - [35] T. Han, M. Hosch, K. Whisnant, B.-L. Young, and X. Zhang, Single top quark production via FCNC couplings at hadron colliders, *Phys. Rev. D* **58**, 073008 (1998), [arXiv:hep-ph/9806486](#).
 - [36] T. Han, K. Whisnant, B. L. Young, and X. Zhang, Top quark decay via the anomalous coupling $\bar{t}c\gamma$ at hadron colliders, *Phys. Rev. D* **55**, 7241 (1997), [arXiv:hep-ph/9603247](#).
 - [37] G. P. G. S. Y. Azatov, Aleksandr Panico, On the flavor structure of natural composite Higgs models and top flavor violation, *Journal of High Energy Physics* **82**, 10.1007/JHEP12(2014)082 (2014).
 - [38] J. Aguilar-Saavedra, Top flavour-changing neutral interactions: theoretical expectations and experimental detection, *Acta Phys. Pol. B* **35**, 2695 (2004).
 - [39] S. L. Glashow, J. Iliopoulos, and L. Maiani, Weak interactions with lepton-hadron symmetry, *Physical review D* **2**, 1285 (1970).
 - [40] M. Schmaltz, D. Stolarski, and J. Thaler, The bestest little higgs, *Journal of High Energy Physics* **2010**, 1 (2010).
 - [41] T. A. Martin and A. de la Puente, Darkening the little higgs, *Physics Letters B* **727**, 443 (2013).
 - [42] K. Moats, *Phenomenology of Little Higgs Models at the Large Hadron Collider*, *Ph.D. thesis* (2012).
 - [43] P. Kalyniak, K. Moats, and T. A. Martin, Constraining the little higgs model of schmaltz, stolarski, and thaler with recent results from the lhc, *Physical Review D* **91**, 013010 (2015).
 - [44] A. M. Sirunyan *et al.* (CMS), A measurement of the Higgs boson mass in the diphoton decay channel, *Phys. Lett. B* **805**, 135425 (2020), [arXiv:2002.06398 \[hep-ex\]](#).
 - [45] V. Shtabovenko, R. Mertig, and F. Orellana, FeynCalc 9.3: New features and improvements, *Computer Physics Communications* **256**, 107478 (2020).
 - [46] H. H. Patel, Package-x: A mathematica package for the analytic calculation of one-loop integrals, *Computer Physics Communications* **197**, 276 (2015).
 - [47] M. Blanke, A. J. Buras, A. Poschenrieder, S. Recksiegel, C. Tarantino, S. Uhlig, and A. Weiler, Rare and CP-violating K and B decays in the Littlest Higgs model with T-parity, *Journal of High Energy Physics* **2007**, 066 (2007).
 - [48] E. Cruz-Albaro and A. Gutiérrez-Rodríguez, Weak dipole moments of the top-quark at the Bestest Little Higgs model, *Eur. Phys. J. Plus* **137**, 1295 (2022), [arXiv:2202.12738 \[hep-ph\]](#).
 - [49] E. Cruz-Albaro, A. Gutiérrez-Rodríguez, J. I. Aranda, and F. Ramírez-Zavaleta, Research on the electromagnetic and weak dipole moments of the tau-lepton at the Bestest Little Higgs Model, *Eur. Phys. J. C* **82**, 1095 (2022), [arXiv:2208.09090 \[hep-ph\]](#).
 - [50] Cruz-Albaro, E. and Gutiérrez-Rodríguez, A. and Hernandez-Ruiz, M. A. and Cisneros-Pérez, T., Searching the anomalous electromagnetic and weak dipole moments of the top-quark at the Bestest Little Higgs Model, [2302.11143 \[hep-ph\]](#).
 - [51] C.-H. Chen, C.-W. Chiang, and C.-W. Su, Top-quark FCNC decays, LFVs, lepton $g-2$, and W mass anomaly with inert charged Higgses 10.48550/arXiv.2301.07070 (2023), [arXiv:2301.07070 \[hep-ph\]](#).
 - [52] J. Carvalho, N. F. Castro, L. Chikovani, T. Djobava, J. Dodd, S. McGrath, A. Onofre, J. Parsons, and F. Veloso, Study of ATLAS sensitivity to FCNC top decays, *Eur. Phys. J. C* **52**, 999 (2007), [arXiv:0712.1127 \[hep-ex\]](#).
 - [53] G. Aad *et al.* (ATLAS), Search for flavour-changing neutral-current interactions of a top quark and a gluon in pp collisions at $\sqrt{s} = 13$ TeV with the ATLAS detector, *Eur. Phys. J. C* **82**, 334 (2022), [arXiv:2112.01302 \[hep-ex\]](#).
 - [54] A. Papaefstathiou and G. Tetlalmatzi-Xolocotzi, Rare top quark decays at a 100 TeV proton-proton collider: $t \rightarrow bWZ$ and $t \rightarrow hc$, *Eur. Phys. J. C* **78**, 214 (2018), [arXiv:1712.06332 \[hep-ph\]](#).

- [55] Particle Data Group and Workman, R. L. et al. , Review of Particle Physics, Progress of Theoretical and Experimental Physics **2022**, [10.1093/ptep/ptac097](#), 083C01.
- [56] R. Sicking, Eva Ström, From precision physics to the energy frontier with the Compact Linear Collider, Nature Physics **16**, [10.1038/s41567-020-0834-8](#) (2020).
- [57] T. K. Charles *et al.* (CLICdp, CLIC), The Compact Linear Collider (CLIC) - 2018 Summary Report **2/2018**, [10.23731/CYRM-2018-002](#) (2018), [arXiv:1812.06018](#) [physics.acc-ph].
- [58] H. A. Ali, N. Arkani-Hamed, I. Banta, S. Benevedes, D. Buttazzo, T. Cai, J. Cheng, T. Cohen, N. Craig, M. Ekhterachian, J. Fan, M. Forsslund, I. G. Garcia, S. Homiller, S. Koren, G. Koszegi, Z. Liu, Q. Lu, K.-F. Lyu, A. Mariotti, A. McCune, P. Meade, I. Ojalvo, U. Oktem, D. Redigolo, M. Reece, F. Sala, R. Sundrum, D. Sutherland, A. Tesi, T. Trott, C. Tully, L.-T. Wang, and M. Wang, The muon smasher's guide, [Reports on Progress in Physics](#) **85**, 084201 (2022).